

Supporting Information

Mechanically Compliant Single Crystals of a Stable Organic Radical

Patrick Commins,^a A. Bernard Dippenaar,^b Liang Li,^a Hideyuki Hara,^c
Delia A. Haynes,^{b,*} Panče Naumov^{a,*}

^a*Smart Materials Lab, New York University Abu Dhabi, PO Box 129188, Abu Dhabi, United Arab Emirates*

^b*Department of Chemistry and Polymer Science, Stellenbosch University, P. Bag X1, Matieland, 7602, Republic of South Africa*

^c*Bruker Japan K.K., 3-9, Moriya, Kanagawa, Yokohama, Kanagawa 221-0022, Japan*

Contents	Page
Supporting Methods.....	S2–S3
Supporting Figures.....	S4–S8

Supporting Methods

Materials preparation. Starting materials and solvents were commercially available, purchased from Sigma-Aldrich South Africa, and used as received. The radical **1** was prepared by using established procedures (Robinson, S. W.; Haynes, D. A.; Rawson, J. M. Co-crystal formation with 1,2,3,5-dithiadiazolyl radicals. *CrystEngComm*, **2013**, *15*, 10205–10211), and purified by vacuum sublimation at 110 °C to yield long, dark needle-shaped crystals.

Quantitative electron paramagnetic resonance (EPR) spectroscopy. Quantitative EPR measurements were acquired at room temperature on a Bruker EMX-nano spectrometer (Bruker BioSpin). Reference free quantitative EPR function was implemented in the Xenon® software package on EMX-nano. The absolute spin value was calculated using pre-defined microwave bridge calibration, resonator profile and measured Q-value and signal integration. The EPR settings were as follows: microwave power, 0.3 mW; total acquisition time, 2 min; magnetic field modulation, 0.4 mT; sweep width, 100 mT.

Electron paramagnetic resonance (EPR) imaging. Images were obtained at room temperature on a Bruker E540 Eleksys EPR spectrometer (Bruker BioSpin), equipped with a TM resonator. For imaging, the system was equipped with water-cooled gradients allowing a magnetic field gradient up to 15 mT/cm along the Y and Z axes. Images were acquired with different sample orientations or positions in order to verify anisotropic effects or field inhomogeneity. 2D images were reconstructed from a complete set of projections, collected as a function of the magnetic field gradient, using the back-projection algorithm implemented in the Xepr® software package. EPR imaging settings were as follows: microwave power, 20 mW; total acquisition time, 10 min; magnetic field modulation, 0.4 mT; sweep width, 170 mT; field of view (FOV) 15 mm; pixel size 0.5 mm; and gradient strength 12 mT/cm.

Powder X-ray diffraction. The measurements were performed in two laboratories:

@Stellenbosch University:

Instrument: Bruker D2 benchtop powder diffractometer
Radiation: Cu
Geometry to record the pattern: Range 2θ 5-40°, rotation at 30 rev/minute
Time of exposure: 1015.5 s
Resolution in 2θ step size: 0.0202064°

Preparation: Unbent crystals were placed on a zero background holder and the pattern recorded. These crystals were then ground with an agate mortar and pestle for 20s under a blanket of nitrogen, and the pattern recorded again.

@New York University Abu Dhabi:

Instrument: Panalytical Empyrean 3 Powder diffractometer
Radiation: Cu
Geometry to record the pattern: Range 2θ 5-50°, rotation at 16 s/rev

Time of exposure: 200.2 s

Resolution in 2θ step size: 0.0262606°

Preparation: The sample(s) were prepared by placing the unbent single crystals on a zero background holder and the pattern was recorded. These crystals were then ground with an granite mortar and pestle for 30s under air and immediately recorded.

Scanning electron microscopy (SEM) and energy dispersive X-ray spectroscopy (EDX). The samples were mounted on a piece of carbon tape and SEM images were obtained using high-vacuum mode on a FEI Quanta 450 Field Emission Scanning Electron Microscope with a primary electron energy of 5 kV and spot size of 2.

Supporting Figures

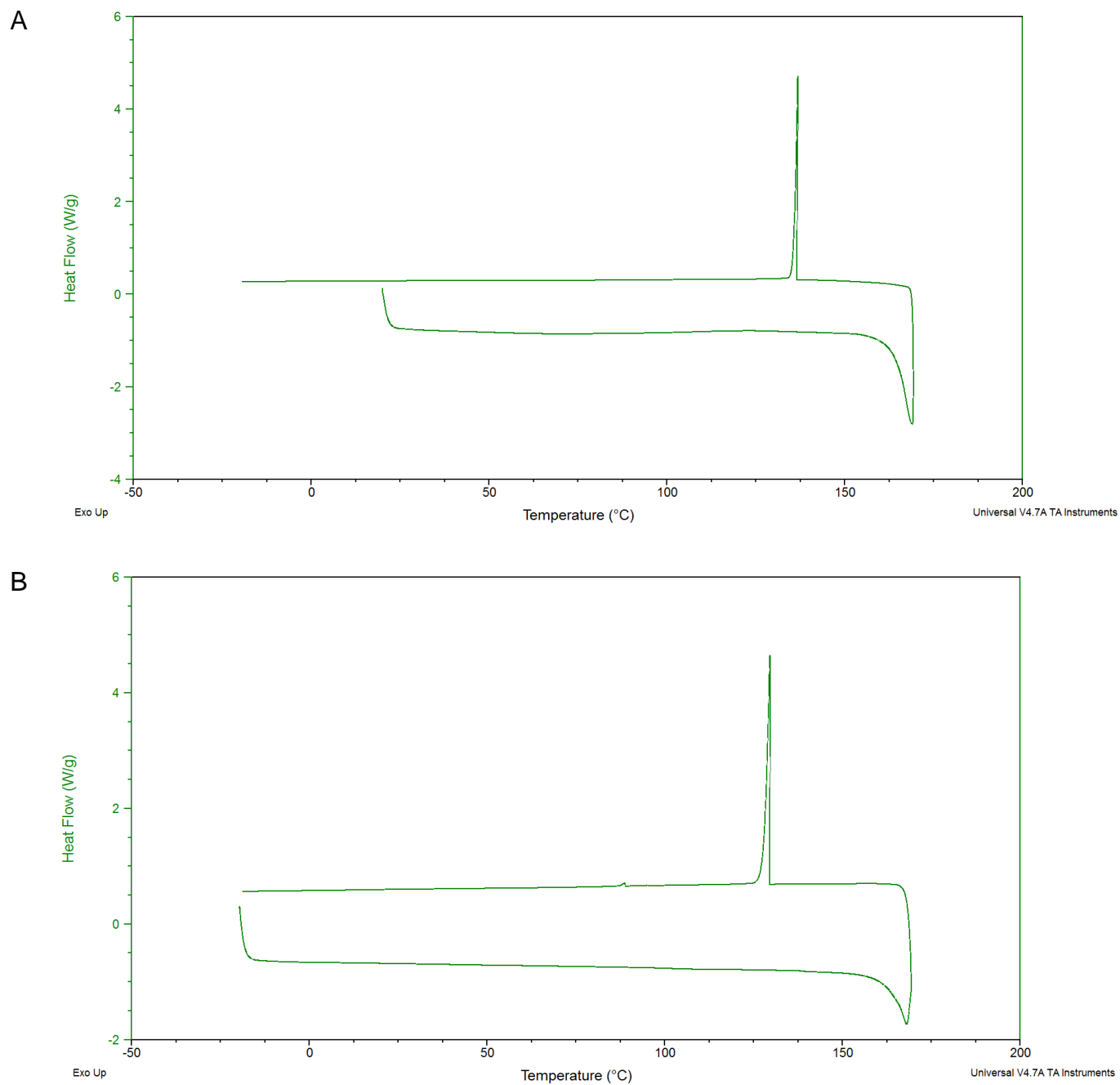


Fig. S1. DSC profile for crystals of **1 β** heated from room temperature to 170 °C at 10 °C/min then cooled to -20 °C at 5 °C/min. A shows the first heating and cooling cycle, B shows the second cycle.

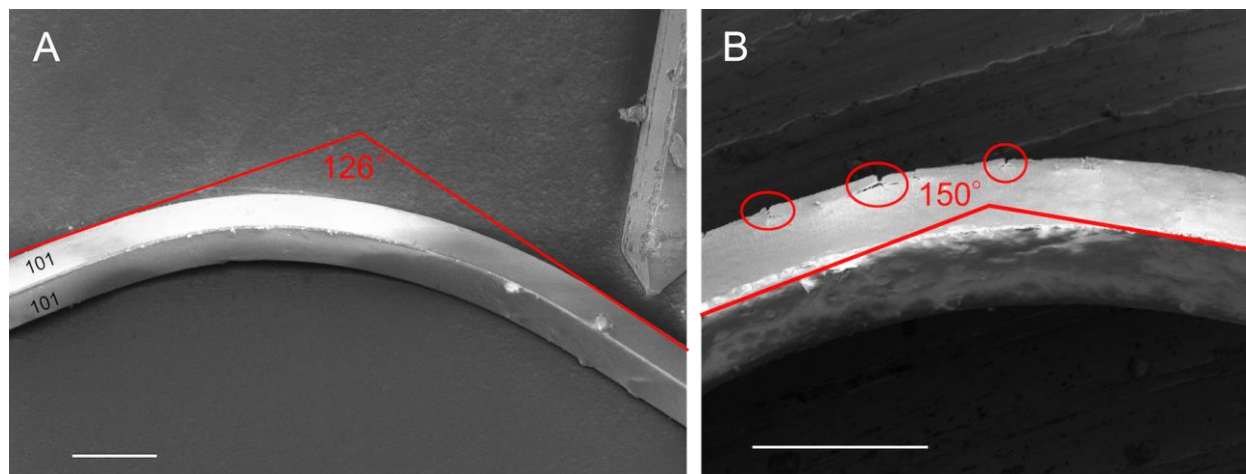


Fig. S2 SEM image of a freshly sublimed bent crystal of **1β** (A), and a crystal of **1β** that was sublimed and then bent two weeks after sublimation indicating its subsequent fracturing (B). Scale bars, A; 100 μm , B; 200 μm .

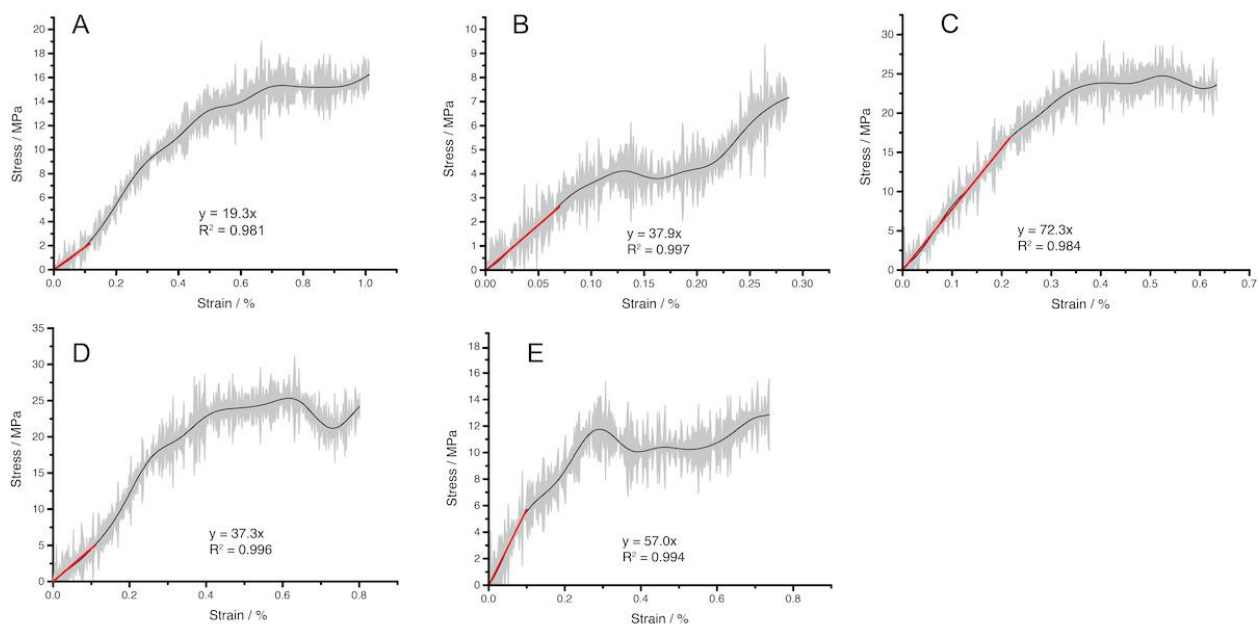


Fig. S3. Stress-strain curves obtained by three-point bending tests on an additional five crystals of **1β**. The error in the measurement is shown as a grey background. The red line indicates the region of the curve that was used to determine the Young's modulus. The slope of the line and linear regression statistics are also shown in each graph.

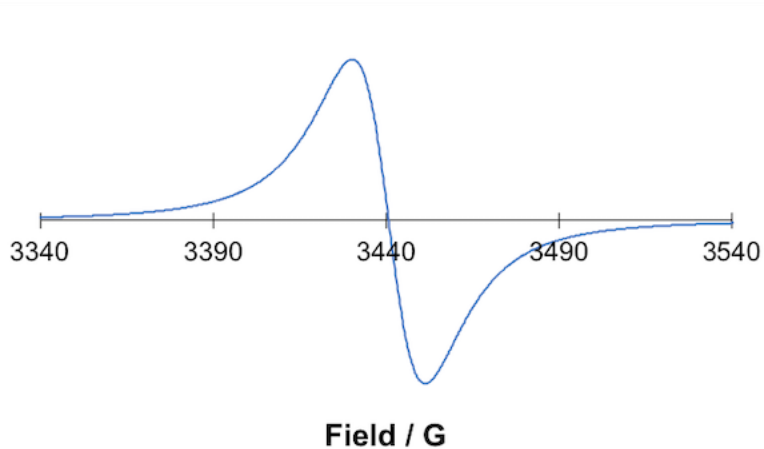


Fig. S4. EPR spectrum of a crystal of the 1β at room temperature.

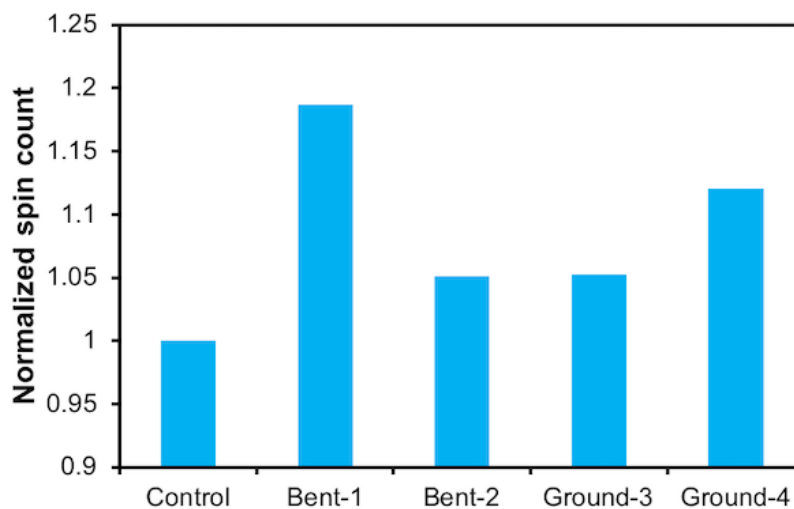


Fig. S5. Normalized spin count after bending or grinding of the crystal of 1β . Each experiment was performed on a different crystal and the values are normalized to the number of spins found in that sample before bending or grinding.

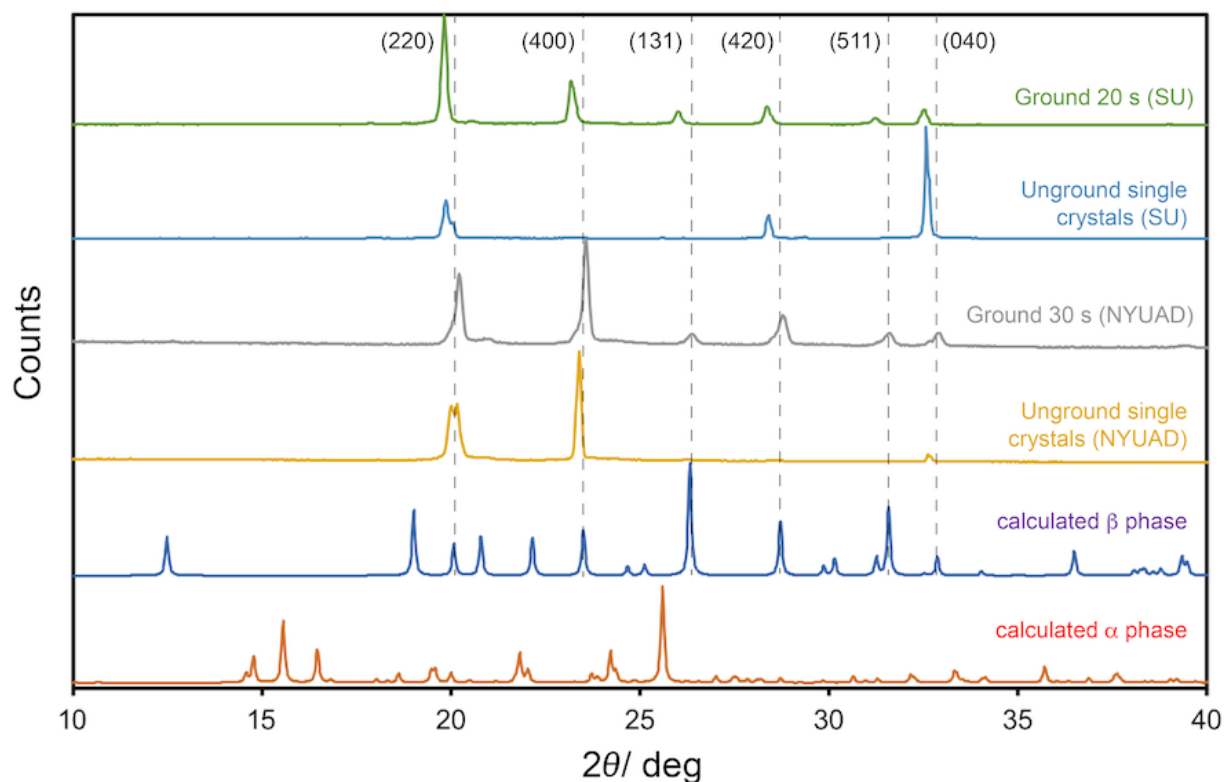


Fig. S6. PXRD analysis of compound **1β** after grinding performed at both New York University Abu Dhabi (NYUAD) and Stellenbosch University (SU). The intensity of all the patterns were normalized using the strongest reflection, and a vertical offset was applied to the individual diagrams for clarity. The discrepancy between the peak intensities of the samples of **1β** used in this work from those of the calculated for phase β is attributed to preferred orientation in these soft, needle-like crystals, similar to what has been reported for other radicals (R. I. Thompson, C. M. Pask, G. O. Lloyd, M. Mito, J. M. R. Rawson, Pressure-induced enhancement of magnetic ordering temperature in an organic radical to 70 K: A magnetostructural correlation. *Chem. Eur. J.*, **2012**, *18*, 8629–8633). The structural and phase identity of the sample was additionally confirmed by single crystal X-ray diffraction.

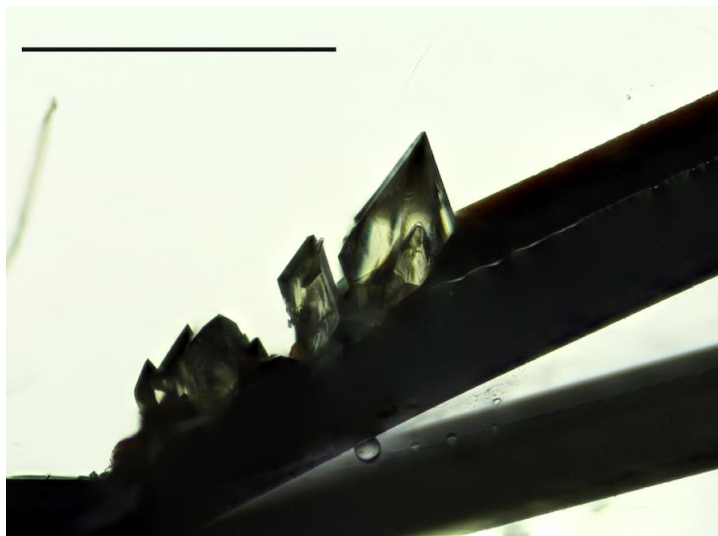


Fig. S7. Optical image of elemental sulfur (S₈) crystals on a crystal of **1β**. Scale bar, 500 μm.